References

[1]R. E. Loehman, M. L. Mecartney, and D. J. Rowcliffe, "Silicon Nitride Joining," Annual Report, AFOSR, Contract F49620-81-K-0001, February 1982.
[2]S. M. Johnson and D. J. Rowcliffe, "Silicon Nitride Joining," Annual Report, AFOSR, Contract F49620-81-K-0001, March 1983.
[3]P. F. Becher and S. A. Halen, "Solid State Bonding of Si_3N_4," *Am. Ceram. Soc. Bull.*, **58** [6] 582-83 (1979).
[4]D. D. Cubicciotti and K. H. Lau, "Kinetics of Oxidation of Hot-Pressed Silicon Nitride Containing Magnesia," *J. Am. Ceram. Soc.*, **61** [11-12] 512-17 (1978).
[5]D. D. Cubicciotti and K. H. Lau, "Kinetics of Oxidation of Yttria Hot-Pressed Silicon Nitride," *J. Electrochem. Soc.*, **126** [10] 1723-28 (1979).
[6]R. E. Loehman, "Basic Research on Oxynitride Glasses," U.S. Army Research Office, Contract DAAG-29-79-C-007, July 1982.
[7]F. F. Lange, "Volatilization Associated with the Sintering of Polyphase Si_3N_4 Materials," *J. Am. Ceram. Soc.*, **65** [8] C-120-C-121 (1982).
[8]C. Greskovich and S. Prochazka, "Stability of Si_3N_4 and Liquid Phases During Sintering," *J. Am. Ceram. Soc.*, **64** [7] C-96-C-97 (1981).
[9]D. L. Hildenbrand, "Mass Spectrometric Studies of Bonding in the Group IIA Fluorides," *J. Chem. Phys.*, **48** [8] 3657-65.
[10]D. L. Hildenbrand, "Dissociation Energies and Chemical Bonding in Alkaline-Earth Chlorides from Mass Spectrometric Studies," *J. Chem. Phys.*, **52** [11] 5751-59 (1970).
[11]R. D. Brittain and D. L. Hildenbrand, "Catalytic Decomposition of Gaseous SO_3," *J. Phys. Chem.*, **87** [19] 3713-17 (1983).
[12]J. B. Mann, "Ionization Cross Sections of the Elements Calculated from Mean-Square Radii of Atomic Orbitals," *J. Chem. Phys.*, **46** [5] 1646-51 (1967).
[13]T. C. Ehlert, "Determination of Transmission Characteristics in Mass Filters," *J. Phys. E.*, **3**, 237 (1970).
[14]S. M. Johnson, R. D. Brittain, R. H. Lamoreaux, and D. J. Rowcliffe, "Cation Transport in Si_3N_4/Glass Couples"; unpublished work.
[15]G. N. Lewis and M. Randall, Thermodynamics, 2d ed. Edited by K. S. Pitzer and L. Brewer. McGraw-Hill, New York, 1961.
[16]D. R. Stull and H. Prophet, JANAF Thermochemical Tables, 2d ed., NSRDS-NOS37, U.S. Government Printing Office, Washington, D.C., 1971, and supplements.
[17]V. P. Glushko, L. V. Gurvich, et al., Thermodynamic Data for Individual Substances, Vol. 4. Institute for High Temperatures, National Academy of Sciences of the U.S.S.R., Moscow, 1983.
[18]G. R. Terwilliger and F. F. Lange, "Pressureless Sintering of Si_3N_4," *J. Mater. Sci.*, **10** [7] 1169-74 (1975).

Preparation of SiO_2 Glass from Model Powder Compacts: I, Formation and Characterization of Powders, Suspensions, and Green Compacts

MICHAEL D. SACKS* and TSEUNG-YUEN TSENG*,*

Department of Materials Science and Engineering, University of Florida, Gainesville, Florida 32611

Dense SiO_2 glass was produced at ≈1000°C by using highly ordered compacts of spherical, nearly monosized, amorphous SiO_2 particles. In Part I of this study, the formation and characterization of powders, suspensions, and green bodies are described. Thermogravimetry and DTA revealed that substantial loss of bound water occurs in powders calcined at temperatures as low as 200°C. Surface area and density measurements were used to show that the water loss occurs without micropore formation. FTIR spectroscopy revealed that residual silanol groups persist to the highest temperatures (1050°C) studied. The state of particulate dispersion in suspensions was modified by pH adjustment and monitored by rheological measurements. Flocculated suspensions (low pH) produce inhomogeneous, low-density powder compacts with highly bimodal pore-size distributions. Uniform green bodies (with higher packing densities) were prepared using well-dispersed suspensions (high pH). Two-dimensional, close-packed hexagonal arrays of particles were observed in these compacts. Pore-size distributions were narrower, but still bimodal due to the presence of three-particle and four-particle pore channels. The sintering behavior of these compacts is described in Part II.

Presented at the 85th Annual Meeting, The American Ceramic Society, Chicago, Illinois, April 26, 1983 (Basic Science Division No. 118-B-83). Received February 14, 1984; revised copy received April 12, 1984; approved May 10, 1984.

Supported by the National Science Foundation (Ceramics Section, Division of Materials Research) under Grant No. DMR-8024320 and by Dresser Industries.

*Member, the American Ceramic Society.

*Now with the Institute of Electronics, National Chiao-Tung University, Hsinchu, Taiwan, Republic of China.

I. Introduction

FUSED SILICA (SiO_2 glass) has many technological applications due to its excellent optical, electrical, and thermal properties. However, traditional melt-based methods of processing are objectionable due to the high temperatures required (≈2000°C). In recent years, flame hydrolysis[1-3] and sol-gel[4-20] methods have been used to produce porous, high specific surface area shapes of amorphous SiO_2. Subsequently, these bodies can be fully densified by sintering (viscous flow mechanism) at relatively low temperatures.[3,9-12,15-17,20,21]

Scherer[2,3] described the sintering behavior of porous SiO_2 "soot" preforms prepared by flame hydrolysis. The preform consists of fine SiO_2 particles produced by oxidation of metal halides (e.g., $SiCl_4$) or organometallic compounds (e.g., methyltri-

methoxysilane) in a gas/oxygen flame. One problem with this method is that particles tend to form large agglomerates. This results in bodies with low green bulk densities and, consequently, large shrinkages occur during sintering. Furthermore, the average pore size is generally several times larger than the average particle size. This partially diminishes the advantage of using high specific surface area, fine-sized particles during sintering since final-stage densification is ultimately controlled by the largest pores present in the microstructure.[22] Nevertheless, sintering to high density was observed at relatively low temperatures (≈1200°C).[3]

Sol-gel processing techniques for preparing porous SiO_2 bodies are often divided into two general methods. In one case (method I), colloidal dispersions (i.e., sols) of fine SiO_2 particles are prepared and subsequently destabilized, or gelled, by chemical and/or thermal treatments.[4–6] The gel is a semirigid, open, three-dimensional network of particles which contains large amounts of interstitial liquid. In method II, organometallic compounds are hydrolyzed and polymerized.[6–20] Gelation occurs as growing polymeric species agglomerate and crosslink to form an extensive, three-dimensional network (which again contains large amounts of interstitial liquid).

To retain monolithic structures after drying, bodies prepared via sol-gel method I are generally processed under conditions which yield large pore sizes compared to method II. Shoup[4] used commercial† fine-particle (≈12 nm diameter, ≈230 m^2/g surface area) sols prepared from soluble silicates to form SiO_2 bodies with various average pore sizes. Only structures with large average pore sizes (≳60 nm) remained monolithic after drying. Rabinovich *et al.*[5] used commercial‡ flame-hydrolyzed SiO_2 particles (≈12 nm diameter, ≈230 m^2/g) to prepare aqueous sols. However, a "double-processing" method, in which large (≈1 to 100 μm) agglomerates were formed, was required to produce gelled monoliths which did not crack on drying. Thus, the advantage of using fine particles for the sintering operation was substantially diminished, while many processing disadvantages associated with the use of agglomerated powders were observed: (1) Green densities were low due to the porous nature of the agglomerates and, consequently, firing shrinkages were large. (2) The green microstructure was inhomogeneous due to the broad size distribution of agglomerates. This probably contributed to severe warping observed in sintered bodies (see Fig. 3 in Ref. 21). (3) Although substantial densification occurred in the temperature range of ≈1200° to 1300°C, optical translucency was not achieved until large interagglomerate pores were eliminated at temperatures of ≈1500°C. Occasional large (≈50 μm) pores still remained in the bodies.

In contrast to sol-gel method I, processing via hydrolysis and condensation polymerization of organometallic compounds (e.g., tetraethylorthosilicate, tetramethylorthosilicate) generally results in bodies with very fine porosity (often ≈2 to 10 nm) and high specific surface area (as high as ≈900 m^2/g).[7,8,11–16,18,20] Consequently, full densification is often achieved at lower temperatures (i.e., in the range 700° to 1200°C).[9–12,15–17,20]

In addition to flame hydrolysis and sol-gel methods, spherical, nearly monosized particles have recently been used to prepare porous SiO_2 bodies for sintering.[23] Particles are produced by hydrolysis of organometallic compounds (e.g., tetraethylorthosilicate) and subsequent condensation/precipitation.[24] Specific surface areas are low and primary particles sizes are large compared to the techniques discussed previously. However, highly ordered, high-density green compacts can be formed using monosized spheres and these bodies sinter at relatively low temperatures (≈1000° to 1100°C).[23]

In the present study, further information is provided on the preparation of SiO_2 glass from compacts of spherical, nearly monosized, amorphous SiO_2 particles. The formation and characterization of powders, suspensions, and green bodies are described in Part I and sintering behavior is reported in Part II.

†Ludox HS-40, E. I. du Pont de Nemours & Co., Inc., Wilmington, DE.
‡Cab-O-Sil M5, Cabot Corp., Boston, MA.

II. Experimental Procedure

(1) Preparation of Materials

Spherical hydrous silica particles with narrow size distribution were produced by the hydrolysis/condensation method of Stober *et al.*[24] Under conditions of constant stirring at room temperature, tetraethylorthosilicate (TEOS)§ [$Si(OC_2H_5)_4$] is added to a solution of reagent-grade ethanol¶ and concentrated (≈30 wt% NH_3) ammonium hydroxide solution.** The TEOS undergoes hydrolysis/condensation reactions, forming (poly)silicic acid. Within minutes, precipitation of uniform spherical particles occurs. By controlling the reactant concentrations,[24] average particle diameters in the range ≈0.2 to 0.6 μm were produced. Particles with an average diameter of ≈0.5 μm were produced using concentrations of ≈3 mol of NH_3/L of ethanol, ≈6.6 mol of H_2O/L of ethanol, and ≈0.25 mol of TEOS/L ethanol.

After precipitation, powders were washed with distilled water and dried. Subsequently, powders were calcined in a loose-stack (uncompacted) arrangement for 24 h at T = 200° to 1050°C (static air atmosphere). All suspensions were prepared with powders which were calcined at 200°C for 24 h. These powders were resuspended in distilled water using ultrasonication†† and pH adjustment (i.e., ammonium hydroxide or hydrochloric acid solutions were added). Green bodies were formed by allowing particles in suspension to settle slowly (under gravitational force) in plastic tubes (≈1 cm diameter). After complete settling, the supernatant liquid was drawn off and the disk-shaped compacts were dried (under ambient conditions) and removed from the tubes.

(2) Characterization of Materials

Powder specific surface area was measured by nitrogen gas adsorption (multipoint BET method).‡‡ Uncalcined powders were vacuum outgassed at room temperature. Calcined samples were outgassed under flowing nitrogen at temperatures in the range ≈80° to 150°C (with lower outgassing temperatures used for powders calcined at lower temperatures). Powder true density was determined by helium gas pycnometry.§§ Differential thermal analysis (DTA) and thermal gravimetric analysis (TG) were carried out in a static air atmosphere at a heating rate of 10°C/min. Infrared spectra were determined on powders by diffuse reflectance Fourier transform infrared (FTIR) spectroscopy.¶¶ Powder X-ray diffraction (XRD) patterns were obtained with a diffractometer*** using Ni-filtered Cu$K\alpha$ radiation and a scanning rate of 6°C/min. Scanning electron microscopy (SEM)††† was also used to characterize powders and powder compacts. A thin gold-palladium coating was deposited on the surface prior to observations in the microscope.

Suspension rheological characteristics (i.e., shear-stress vs shear-rate behavior) were determined with a concentric cylinder viscometer.‡‡‡ Viscosity values were obtained from the flow curves. Suspension electrokinetic behavior was determined using a microelectrophoresis apparatus.§§§ A minimum of 20 individual mobility measurements was averaged for each sample. Zeta potentials were determined using the electrophoretic mobilities and the Helmholtz-Smoluchowski equation[25]:

$$\zeta = \mu\eta/\varepsilon\varepsilon_0 \tag{1}$$

where ζ = zeta potential in V, μ = electrophoretic mobility in $m^2 \cdot s^{-1} \cdot V^{-1}$, η = viscosity of the suspending liquid in Pa·s, ε = relative dielectric constant of the suspending liquid, and ε_0 = permittivity of vacuum (8.854×10^{-12} F/m).

The bulk density of the disk-shaped green bodies was determined from measurements of sample weight and geometric

§Fisher Scientific Co., Fair Lawn, NJ.
¶Fisher Scientific Co.
**Fisher Scientific Co.
††Model W-375, Heat Systems-Ultrasonics, Inc., Farmingdale, NY.
‡‡Model OS-7, Quantachrome Corp., Syosset, NY.
§§Model PY-5, Quantachrome Corp.
¶¶Model MX-1, Nicolet Analytical Co., Madison, WI.
***Model APD 3520, Philips Electronic Instruments Co., Mt. Vernon, NY.
†††Model JSM-35C, Japan Electron Optics Co., Ltd., Tokyo, Japan.
‡‡‡Model RV-100/CV-100 viscometer, Haake Inc., Saddle Brook, NJ.
§§§Mark II, Rank Brothers, Cambridge, England.

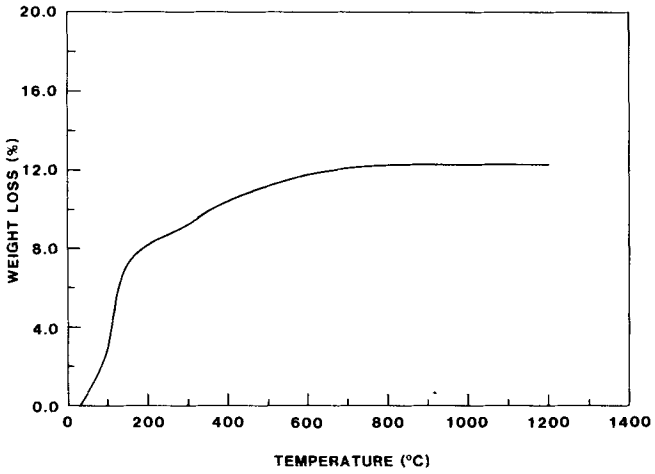

Fig. 1. TG curve for uncalcined SiO_2 powder.

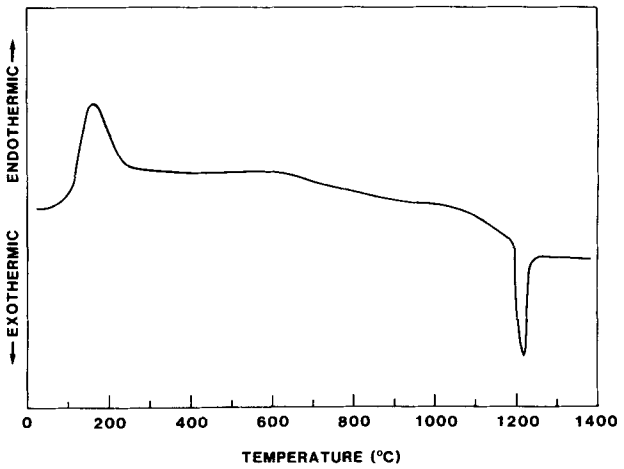

Fig. 3. DTA curve for uncalcined SiO_2 powder.

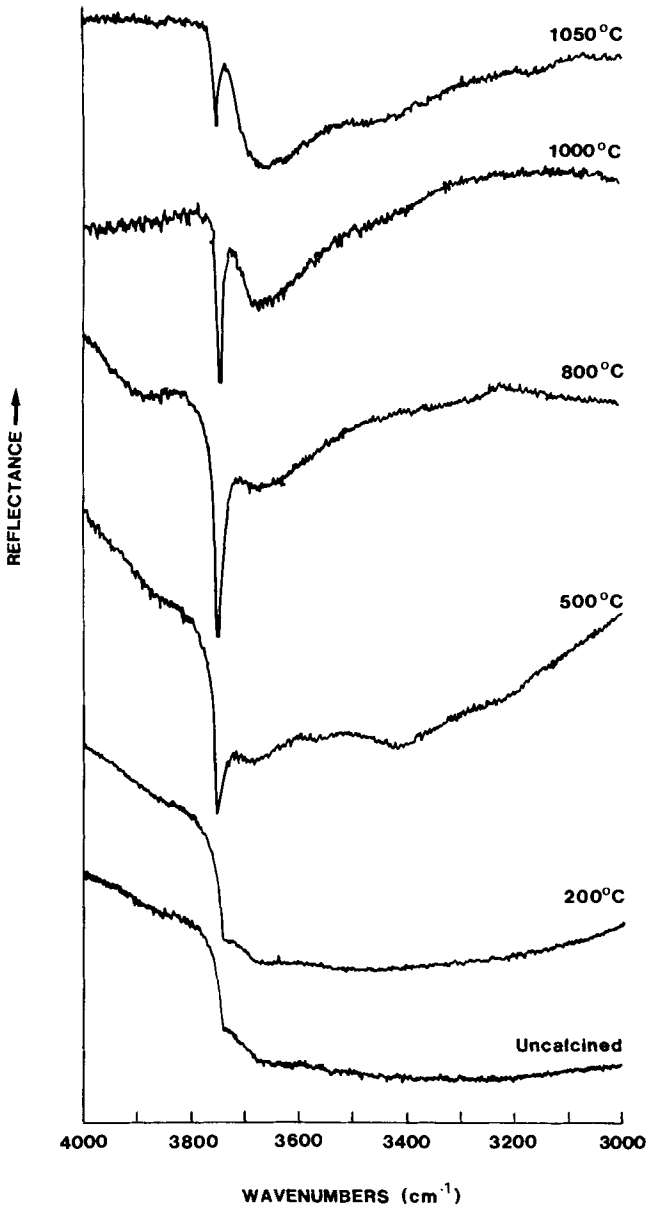

Fig. 2. FTIR spectra for SiO_2 powders calcined for 24 h at temperatures indicated.

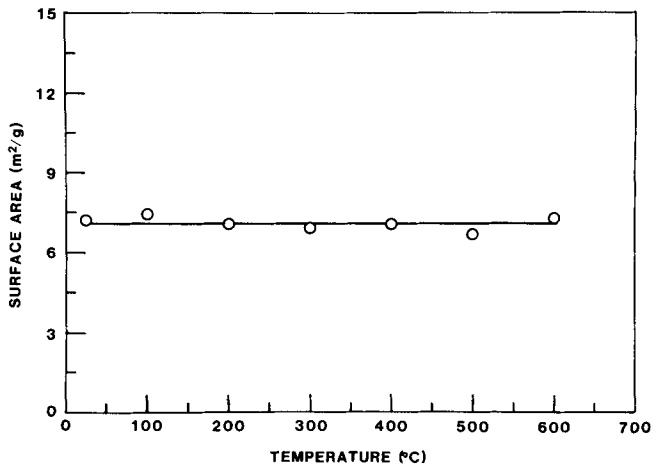

Fig. 4. Specific surface area for SiO_2 powders calcined for 24 h at temperatures indicated.

dimensions. (Abrasive papers were used to improve flatness and parallelism of the faces of the dried disks.) Information on pore-size distributions was obtained by scanning mercury porosimetry.[¶¶¶] The specific volume distribution of pore radii was determined by applying the Washburn equation for liquid penetration into a cylindrical capillary (i.e., pore). Standard values were used for the mercury surface energy (0.484 J/m^2) and the contact angle on the solid (θ = 140°).

III. Results and Discussion

(1) Powder Characterization

Thermogravimetry (Fig. 1) shows that ≈12% total weight loss occurs on heating. The FTIR results (Fig. 2) indicate that the weight loss is primarily associated with the removal of hydration water and hydroxyl groups. The very broad absorption band observed over the range ≈3000 to 3600 cm^{-1} in the uncalcined material is associated with the O–H stretching vibrations in hydrogen-bonded molecular water (symmetric ν_1 and anti-

[¶¶¶]Model SP-100, Quantachrome Corp.

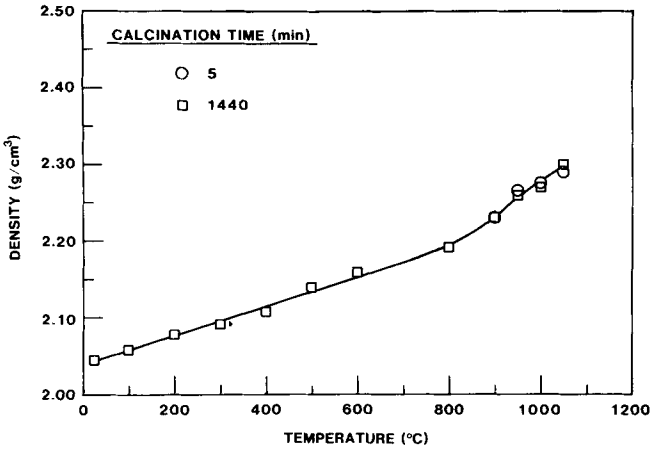

Fig. 5. Gas pycnometry density vs calcining temperature for SiO_2 powders calcined for times indicated.

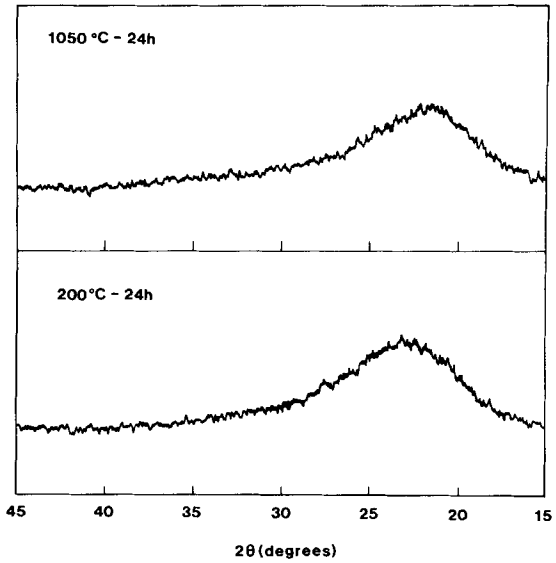

Fig. 6. XRD patterns for SiO_2 powders calcined for 24 h at temperatures indicated.

symmetric ν_3) and in silanol groups (Si–OH) bonded to molecular water.[26] The absorption centered at ≈3660 cm^{-1} and the shoulder at ≈3740 cm^{-1} are associated with O–H stretching vibrations for hydrogen-bonded silanol groups and "free," or isolated, silanol groups, respectively.[26] As the calcination temperature is increased, molecular water and hydroxyl groups are removed from the silica. The rapid initial weight loss (Fig. 1) and the endothermic peak (centered at ≈160°C) observed in DTA (Fig. 3) indicate that much of the bound water can be eliminated at temperatures as low as 200°C. The FTIR spectra show that essentially all the bound water associated with the broad absorption band in the uncalcined material is removed by 800°C (i.e., approximately the same temperature at which the TG curve levels off). However, it is clear that "free" silanol groups (peak at ≈3750 cm^{-1} in the FTIR spectra) and hydrogen-bonded silanol groups (peak at ≈3670 cm^{-1} in the FTIR spectra) persist to the highest temperatures studied.

Dehydroxylation reactions are often accompanied by micropore formation and concomitant increases in specific surface area.[27,28] However, in the present study, micropore formation does not occur since no significant changes were observed in powder specific surface area with increasing calcination temperature (Fig. 4). Furthermore, the measured surface areas (≈7 m^2/g) are in good agreement with values (≈6 m^2/g) calculated from the average particle diameter and the powder true density. (The powder used in Fig. 4 had an average diameter of ≈0.5 μm, as measured from electron micrographs. Powder true densities are given in Fig. 5.)

Dehydroxylation is accompanied by small increases in true density with increasing calcination temperature (Fig. 5). These measurements were made on powders which were calcined in a loose-stack (uncompacted) arrangement. Even at the highest calcination temperature (1050°C), powders still retained the character of a loose stack (as opposed to becoming a sintered mass). This indicated that sintering had not progressed beyond the initial stage and that there are no closed pores as a result of sintering. Therefore, gas pycnometry measurements in Fig. 5 represent true densities (as opposed to apparent densities).

Density values for powders calcined at $T > 800$°C are slightly higher than the value (2.20 g/cm^3) usually reported for fused SiO_2.[6] One explanation given consideration is that the material transforms from the amorphous state to a higher-density crystalline phase (e.g., cristobalite with a density[6] of 2.32 g/cm^3). However, the exothermic peak in DTA (Fig. 3) indicates that devitrification does not occur until ≈1200°C. This is confirmed by XRD measurements (Fig. 6) which show that very little change occurs up to temperatures of 1050°C for powders calcined in a loose-stack arrangement. The extensive broadening observed in each sample (centered at $2\theta \approx 22°$) is characteristic of amorphous silica.[29] Another possible explanation, suggested by previous investigators,[6,30]

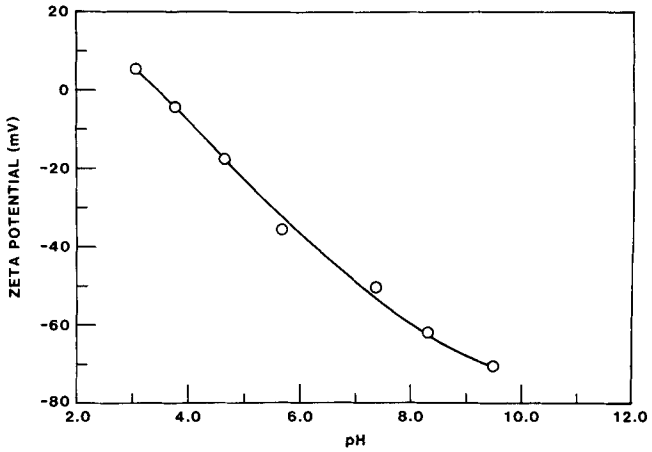

Fig. 7. Plot of zeta potential vs pH for silica.

is that structural rearrangements leading to a more ordered, dense packing of SiO_4 tetrahedra occur prior to devitrification, but that the scale of ordering is too small to be detected by ordinary XRD procedures. Further study would be required to confirm this interpretation.

(2) Suspension Characterization

Powders were calcined at 200°C for 24 h prior to suspension preparation for two reasons. First, powders calcined at 200°C still have sufficient surface hydroxylation to be readily wet by water. In contrast, powders calcined at 500°C, for example, are sufficiently hydrophobic to make aqueous suspension preparation difficult. Second, weight losses during subsequent heat treatment of green bodies are small because the calcined powders contain only ≈2% residual bound water.

The state of particulate dispersion in suspension was varied by pH adjustment and monitored by rheological measurements. Electrokinetic measurements (Fig. 7) revealed that zeta potentials (absolute values) vary by ≈70 mV over the pH range ≈3 to 10. (With other factors constant, better dispersion is obtained when particles have high zeta potentials, since electrostatic repulsion forces between particles are increased.) Figure 8 shows that the viscosity is independent of shear rate (i.e., Newtonian behavior) in a pH = 10

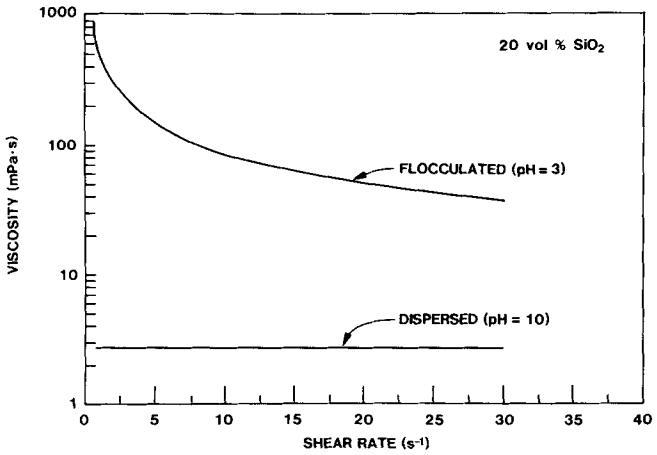

Fig. 8. Plots of suspension viscosity vs shear rate for dispersed (pH = 10) and flocculated (pH = 3) suspensions.

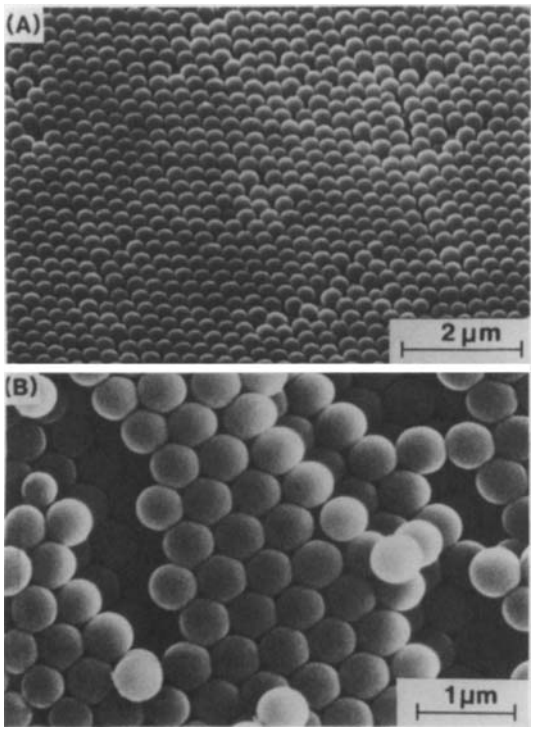

Fig. 9. Scanning electron micrographs of compacts containing close-packed planes. Samples were prepared from dispersed suspensions of particles (*A*) ≈0.35 μm and (*B*) ≈0.5 μm in diameter.

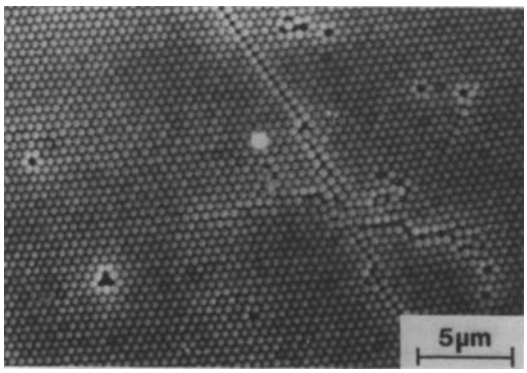

Fig. 10. Scanning electron micrograph showing defects in ordered compact.

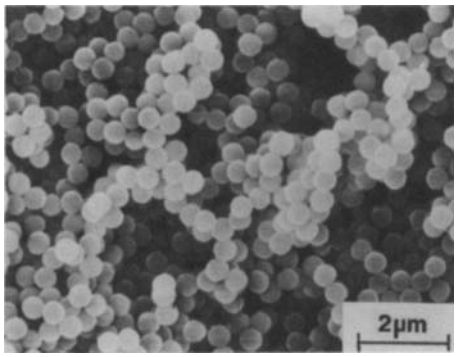

Fig. 11. Scanning electron micrograph of compact prepared from flocculated suspension.

suspension (20 wt% solids content). In contrast, the viscosity in a pH = 3 suspension decreases rapidly with increasing shear rate (Fig. 8), i.e., highly shear thinning behavior. The Newtonian behavior and low viscosity observed at pH = 10 are characteristic of a well-dispersed suspension. The shear thinning flow and high viscosities observed at pH = 3 indicate that the suspension is highly flocculated. In flocculated suspensions, liquid is immobilized in interparticulate pore channels of the floc networks (i.e., the "effective" solids loading is increased relative to dispersed system). Shear thinning flow results from the breakdown of the flocculated structure (and the release of entrapped liquid).

(3) Green Compact Characterization

Green bodies prepared by particle sedimentation from well-dispersed suspensions contain two-dimensional, close-packed hexagonal arrays of particles (Fig. 9). These planes contain defects (Fig. 10) which are analogous to vacancies, dislocations, grain boundaries, etc. in atomic crystalline structures. Ordered regions may extend tens of micrometers before "grain," or domain, boundaries are observed. In contrast, bodies prepared from flocculated suspensions do not show extensive ordering (Fig. 11). However, individual flocs appear to have a high packing density (Fig. 11).

Plots of the specific pore volume frequency function, $f_v(r)$, vs pore radius, r, are shown in Fig. 12 for compacts prepared from dispersed and flocculated suspensions. As expected, the compact prepared from the flocculated suspension (≈0.5 μm particle diameter) has a highly bimodal pore-size distribution. The compact contains smaller intrafloc pores (mode size ≈50 nm) and larger interfloc pores (mode size ≈120 nm). The narrow distribution of interfloc pores suggests that the flocs have a fairly uniform size distribution. The mode size for the intrafloc pores is relatively small, i.e., approximately the same as the mode size for the smaller pores in the high-density, ordered sample prepared from the dispersed suspension (Fig. 12). This indicates that primary particles form dense packing arrangements in the flocs.

Compared to the sample formed from the flocculated suspension, the ordered compact has a narrower pore-size distribution (Fig. 12). However, the distribution is still bimodal. In this case, the bimodality arises due to two types of pore channels in the ordered structure; i.e., channels may be surrounded by three or four particles (Fig. 13). From the average particle diameter (≈0.5 μm for the compact used in Figs. 12 and 13), the calculated channel radii are 39 and 104 nm for three-particle and four-particle channels, respectively. These values are in reasonable agreement with the observed mode sizes of ≈50 and ≈80 nm (Fig. 12).

The observation of ordered, close-packed planes (Figs. 9 and 10) does not necessarily imply the existence of three-dimensional regions of close packing. Furthermore, the observation (Fig. 13) of two types of ordered planes (i.e., planes with (1) three-particle pore channels and (2) four-particle pore channels) is not unique to close-packed structures. At the present time, the type of packing structure is uncertain. However, several observations of interest are noted:

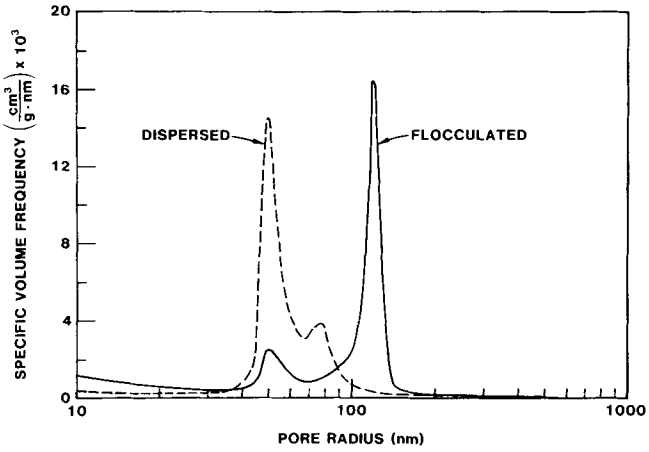

Fig. 12. Plots of specific pore volume frequency function, $f_v(r)$, vs pore radius, r, for compacts prepared from dispersed and flocculated suspensions.

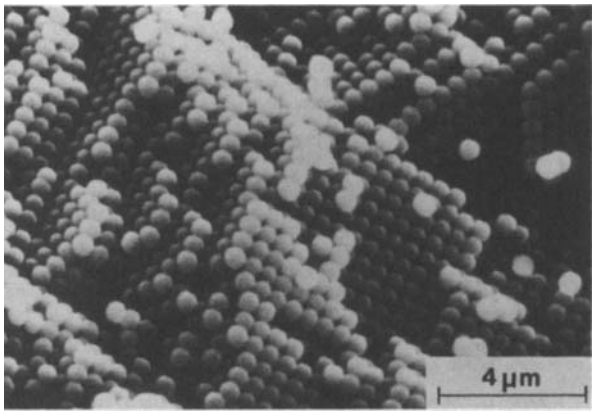

Fig. 13. Scanning electron micrograph showing three-particle and four-particle pore channels in ordered compact.

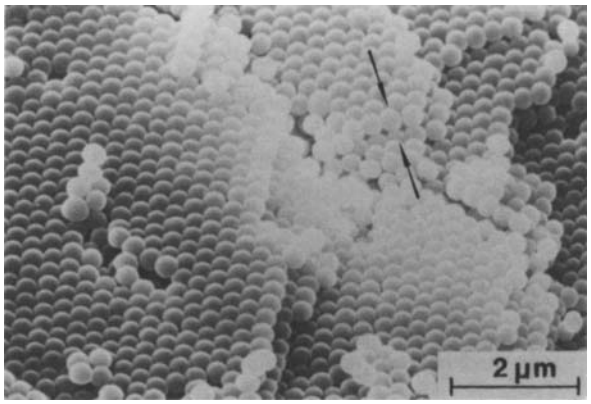

Fig. 14. Scanning electron micrograph showing "simple hexagonal" structure in which close-packed planes stack directly on top of each other.

(1) Figure 14 shows an SEM fracture surface of a compact prepared from a suspension of well-dispersed, ≈0.35-μm diameter, particles. In several areas (note arrows), it is evident that close-packed planes stack directly on top of each other, i.e., a "simple hexagonal" packing. Although most studies of colloid "crystals" have reported face-centered cubic or body-centered cubic structures,[31] a study by Hoffman[32] suggests that the formation of a "simple hexagonal" structure may be possible. Using light-diffraction measurements, he concluded that *two-dimensional* hexagonal arrays existed in concentrated suspensions of monosized, spherical poly(vinyl chloride) particles.

(2) The average green compact density (for ≈25 samples) was 59.5 ± 0.8%, i.e., considerably below the value of ≈74% for three-dimensional close-packed structures. It seems unlikely that packing defects (e.g., vacancies, "grain" boundaries, etc.) account for the entire difference. This suggests that lower-density packing structures (e.g., "simple" hexagonal, body-centered cubic, etc.) are important in these compacts.

IV. Conclusion

Spherical, nearly monosized particles of hydrous SiO_2 were prepared by the method of Stober *et al.*[24] Thermogravimetry and DTA revealed that substantial loss of bound water occurred at temperatures as low as 200°C. However, FTIR spectroscopy showed that residual silanol groups persist to the highest temperature (1050°C) studied. Powder true density was observed to increase with the removal of chemically bound water. Density values greater than 2.20 g/cm^3 (i.e., the density of fused silica) were obtained at $T > 800$°C, yet X-ray diffraction patterns were characteristic of amorphous silica. Further study is required to explain this behavior.

Green compacts were prepared by sedimentation of particles from suspensions. The state of particulate dispersion in suspension was modified by pH adjustment. Flocculated suspensions (low pH) show shear thinning behavior, high viscosity, and a nearly zero zeta potential. These suspensions produce powder compacts with highly bimodal pore-size distributions (i.e., due to intra- and interfloc pores). In contrast, well-dispersed suspensions (high pH) show Newtonian behavior, low viscosity, and a large negative zeta poential. Highly ordered compacts are produced from these suspensions. Pore-size distributions are narrower, but still bimodal due to the presence of both three-particle and four-particle pore channels.

Two-dimensional hexagonal arrays of particles (close-packed planes) were observed in the highly ordered compacts. Defects analogous to vacancies, dislocations, grain boundaries, etc., in atomic crystalline structures were also observed. At the present time, the three-dimensional structure of these compacts is uncertain. Light diffraction studies may be helpful in elucidating the packing structure.

Acknowledgments: The authors thank A. Tomsia of Lawrence Berkeley Laboratory for the TG and DTA and C. Khadilkar, G. Scheiffele, O. Rojas, T. S. Yeh, and E. Clausen of the University of Florida for experimental assistance.

References

[1]P. C. Shultz, "Optical Absorption of the Transition Elements in Vitreous Silica," *J. Am. Ceram. Soc.*, **57** [7] 309–13 (1974).
[2]G. W. Scherer, "Sintering of Low-Density Glasses: I, Theory," *J. Am. Ceram. Soc.*, **60** [5–6] 236–39 (1977).
[3]G. W. Scherer, "Sintering of Low-Density Glasses: II, Experimental Study," *J. Am. Ceram. Soc.*, **60** [5–6] 239–43 (1977).
[4]R. D. Shoup, "Controlled Pore Silica Bodies Gelled from Silica Sol-Alkali Silicate Mixtures"; pp. 63–69 in Colloid and Interface Science, Vol. III. Edited by M. Kerker. Academic Press, New York, 1976.
[5]E. M. Rabinovich, D. W. Johnson, Jr., J. B. MacChesney, and E. M. Vogel, "Preparation of High Silica Glasses from Colloidal Gels: I, Preparation for Sintering and Properties of Sintered Glasses," *J. Am. Ceram. Soc.*, **66** [10] 683–88 (1983).
[6]R. K. Iler, The Chemistry of Silica. Wiley & Sons, New York, 1979.
[7]B. E. Yoldas, "Preparation of Glasses and Ceramics from Metal-Organic Compounds," *J. Mater. Sci.*, **12**, 1203–08 (1977).
[8]M. Yamane, S. Aso, and T. Sakaino, "Preparation of a Gel from Metal Alkoxide and Its Properties as a Precursor Oxide," *J. Mater. Sci.*, **13**, 865–70 (1978).
[9]S. Sakka and K. Kamiya, "Preparation of Compact Solids from Metal Alkoxides"; pp. 101–109 in Proceedings of International Symposium of Factors in Densification and Sintering of Oxide and Non-Oxide Ceramics. Edited by S. Somiya and S. Saito. Tokyo Institute of Technology, Tokyo, Japan, 1978.
[10]M. Yamane, S. Aso, S. Okano, and T. Sakaino, "Low Temperature Synthesis of a Monolithic Silica Glass by the Pyrolysis of a Silica Gel," *J. Mater. Sci.*, **14**, 607–11 (1979).

[11]M. Nogami and Y. Moriya, "Glass Formation Through Hydrolysis of $Si(OC_2H_5)_4$ with NH_4OH and HCl Solution," *J. Non-Cryst. Solids*, **37**, 191–201 (1980).
[12]K. Susa, I. Matsuyama, S. Satoh, and T. Suganuma, "New Optical Fiber Fabrication Method," *Electron. Lett.*, **18** [12] 499–500 (1982).
[13]L. C. Klein and G. J. Garvey, "Monolithic Dried Gels," *J. Non-Cryst. Solids*, **48**, 97–104 (1982).
[14]J. Zarzycki, M. Prassas, and J. Phalippou, "Synthesis of Glasses from Gels: the Problem of Monolithic Gels," *J. Mater. Sci.*, **17**, 3371–79 (1982).
[15]C. J. Brinker, K. D. Keefer, D. W. Schaeffer, and C. S. Ashley, "Sol-Gel Transition in Simple Silicates," *J. Non-Cryst. Solids*, **48**, 47–64 (1982).
[16]L. C. Klein and G. J. Garvey, "Drying and Firing Monolithic Silica Shapes from Sol-Gels"; pp. 88–99 in Ultrastructure Processing of Ceramics, Glasses, and Composites. Edited by L. L. Hench and D. R. Ulrich. Wiley & Sons, New York, 1984.
[17]M. Prassas and L. L. Hench, "Physical Chemical Factors in Sol-Gel Processing"; pp. 100–125 in Ultrastructure Processing of Ceramics, Glasses, and Composites. Edited by L. L. Hench and D. R. Ulrich. Wiley & Sons, New York, 1984.
[18]C. J. Brinker and G. W. Scherer, "Relationships Between Sol-to-Gel and Gel-to-Glass Conversions"; pp. 43–59 in Ultrastructure Processing of Ceramics, Glasses, and Composites. Edited by L. L. Hench and D. R. Ulrich. Wiley & Sons, New York, 1984.
[19]J. Zarzycki, "Monolithic Xero and Aerogels for Gel-Glass Processes"; pp. 27–42 in Ultrastructure Processing of Ceramics, Glasses, and Composites. Edited by L. L. Hench and D. R. Ulrich. Wiley & Sons, New York, 1984.
[20]J. Phalippou, T. Woigner, and J. Zarzycki, "Behavior of Monolithic Silica Aerogels at Temperatures Above 1000°C"; pp. 70–87 in Ultrastructure Processing of Ceramics, Glasses, and Composites. Edited by L. L. Hench and D. R. Ulrich. Wiley & Sons, New York, 1984.
[21]D. W. Johnson, Jr., E. M. Rabinovich, J. B. MacChesney, and E. M. Vogel, "Preparation of High-Silica Glasses from Colloidal Gels: II, Sintering," *J. Am. Ceram. Soc.*, **66** [10] 688–93 (1983).
[22]M. D. Sacks and J. A. Pask, "Sintering of Mullite-Containing Materials: II, Effect of Agglomeration," *J. Am. Ceram. Soc.*, **65** [2] 70–77 (1982).
[23]T. Shimohira, A. Makishima, K. Kotani, and M. Wakakuwa, "Sintering of Monodispersed Amorphous Silica Particles"; pp. 119–27 in Proceedings of the International Symposium of Factors in Densification and Sintering of Oxide and Non-Oxide Ceramics. Edited by S. Somiya and S. Saito. Tokyo Institute of Technology, Tokyo, Japan, 1978.
[24]W. Stober, A. Fink, and E. Bohn, "Controlled Growth of Monodisperse Silica Spheres in the Micron Size Range," *J. Colloid Interface Sci.*, **26**, 62–69 (1968).
[25]J. Th. G. Overbeek, "The Interaction Between Colloid Particles"; pp. 245–77 in Colloid Science. Edited by H. R. Kruyt. Elsevier, Amsterdam, 1952.
[26]M. L. Hair, Infrared Spectroscopy in Surface Chemistry. Marcel Dekker, New York, 1975.
[27]S. J. Wilson and M. H. Stacey, "The Porosity of Aluminum Oxide Phases Derived from Well-Crystallized Boehmite: Correlated Electron Microscope, Adsorption, and Porosimetry Studies," *J. Colloid Interface Sci.*, **82** [2] 507–17 (1981).
[28]S. J. Wilson and J. D. C. McConnell, "Energetics of Formation of Lamellar Porous Microstructures in γ-Al_2O_3," *J. Mater. Sci.*, **15**, 3081–90 (1980).
[29]W. D. Kingery, H. K. Bowen, and D. R. Uhlmann, Introduction to Ceramics, 2d ed. Wiley & Sons, New York, 1976.
[30]J. Fraissard and B. Imelik, "The Structure and the Sintering of Silica Gels," *J. Chim. Phys.*, **59**, 415–18 (1962).
[31]P. Pieranski, "Defects in Three and Two-Dimensional Colloidal Crystals"; pp. 183–200 in Physics of Defects. Edited by M. Kleman. North-Holland, Amsterdam, 1980.
[32]R. L. Hoffman, "Discontinuous and Dilatant Viscosity Behavior in Concentrated Suspensions. I. Observations of a Flow Instability," *Trans. Soc. Rheol.*, **16** [1] 155–73 (1972).

Preparation of SiO_2 Glass from Model Powder Compacts: II, Sintering

MICHAEL D. SACKS* and TSEUNG-YUEN TSENG*,*

Department of Materials Science and Engineering, University of Florida, Gainesville, Florida 32611

The sintering behavior of powder compacts formed from spherical, nearly monosized SiO_2 particles was investigated. Highly ordered compacts sintered to high density and translucency at 1000°C. In contrast, less homogeneous samples prepared from flocculated suspensions remained highly porous after sintering under the same conditions. Densification kinetics were determined over the temperature range 900° to 1050°C for ordered compacts. The viscosity at each sintering temperature and the activation energy for viscous flow were determined using available sintering models. Sintering of ordered compacts is divided into several stages. Densification, mercury porosimetry, and electron microscopy results indicate that the first stage is dominated by the shrinkage of three-particle pore channels, whereas the second stage primarily involves the shrinkage of four-particle pore channels.

I. Introduction

QUANTITATIVE prediction of sintering behavior is a difficult task, primarily due to the enormously complex geometrical changes that occur during the process. Many of these geometrical complexities are associated with the nonideal structure of most powders and powder compacts. First, powders usually have a wide range of particle sizes and shapes. This leads to complex particle-particle contact geometries and complex pore geometries. Second, powders are often agglomerated. This results in differential microdensification rates during the sintering of powder compacts. Simultaneously, certain regions are undergoing final-stage sintering (i.e., densification is nearly complete and, for crystalline materials, grain growth has occurred), while other regions are in the initial stage of sintering (i.e., only neck formation has occurred).[1] Even with spherical particles of uniform size, rearrangement processes can occur if packing inhomogeneities exist.[2,3]

Based on the above considerations, the ideal powder compact for sintering studies would consist of monosized particles of

Presented at the 85th Annual Meeting, The American Ceramic Society, Chicago, Illinois, April 26, 1983 (Basic Science Division No. 118–B–83). Received February 14, 1984; revised copy received April 12, 1984; approved May 10, 1984.
Supported by the National Science Foundation (Ceramics Section, Division of Materials Research) under Grant No. DMR–8024320 and by Dresser Industries.
*Member, the American Ceramic Society.
*Now with the Institute of Electronics, National Chiao-Tung University, Hsinchu, Taiwan, Republic of China.